JOURNAL OF GEOPHYSICAL RESEARCH, VOL. 108, NO. B5, 2273, doi:10.1029/2001JB001741, 2003

Landscape evolution at extensional relay zones

Alexander L. Densmore,[1] Nancye H. Dawers,[2] Sanjeev Gupta,[3] Philip A. Allen,[1] and Ruth Gilpin[4]

Received 29 December 2001; revised 24 January 2003; accepted 20 February 2003; published 24 May 2003.

[1] It is commonly argued that the extensional relay zones between adjacent crustal-scale normal fault segments are associated with large catchment-fan systems that deliver significant amounts of sediment to hanging wall basins. This conceptual model of extensional basin development, while useful, overlooks some of the physical constraints on catchment evolution and sediment supply in relay zones. We argue that a key factor in the geomorphic evolution of relay zones is the interplay between two different timescales, the time over which the fault array develops, and the time over which the footwall catchment-fan systems are established. Results of numerical experiments using a landscape evolution model suggest that, in isolated fault blocks, footwall catchment evolution is highly dependent on the pattern and rate of fault array growth. A rapidly linked en echelon fault geometry gives rise to capture of relay zone drainage by aggressive catchment incision in the relay zone and to consequent increases in the rate of sediment supply to the hanging wall. Capture events do not occur when the fault segments are allowed to propagate slowly toward an en echelon geometry. In neither case, however, are large relay zone catchment-fan systems developed. We propose several physical reasons for this, including geometric constraints and limits on catchment incision and sediment transport rates in relay zones. Future research efforts should focus on the timescales over which fault array development occurs, and on the quantitative variations in catchment-fan system morphology at relay zones. *INDEX TERMS:* 1824 Hydrology: Geomorphology (1625); 1815 Hydrology: Erosion and sedimentation; 3210 Mathematical Geophysics: Modeling; 8010 Structural Geology: Fractures and faults; 8109 Tectonophysics: Continental tectonics—extensional (0905); *KEYWORDS:* normal faults, numerical models, relay zones, landscape evolution

Citation: Densmore, A. L., N. H. Dawers, S. Gupta, P. A. Allen, and R. Gilpin, Landscape evolution at extensional relay zones, *J. Geophys. Res.*, *108*(B5), 2273, doi:10.1029/2001JB001741, 2003.

1. Introduction

[2] Continental crustal-scale normal faults typically occur as a series of segments of lengths that scale approximately with the thickness of the brittle crust [*Jackson and White*, 1989; *Wallace*, 1989a]. At their endpoints, adjacent segments interact through a variety of geometric structures and mechanical processes. The most common geometry is that of overlapping en echelon segments linked through relay zones (Figure 1), which transfer displacement between adjacent segments [e.g., *Larsen*, 1988]. These relay zones are places of anomalous footwall and hanging wall topography because of the distributed nature of strain accommodation. Relay zones have attracted considerable research interest, partly because they are critical areas for understanding how fault segments coalesce to form large fault arrays, and also because of the possible role they play in sediment transport to extensional basins. A number of studies have argued that (1) large catchments occur in relay zones and are capable of collecting and transporting significant volumes of sediment from the footwall and (2) this sediment is delivered to large fans adjacent to the zones [e.g., *Leeder and Gawthorpe*, 1987; *Gawthorpe and Hurst*, 1993; *Leeder and Jackson*, 1993; *Eliet and Gawthorpe*, 1995; *Ravnås and Steel*, 1998; *Gupta et al.*, 1999; *Gawthorpe and Leeder*, 2000]. This model is consistent with some field examples in active extensional basins in the Basin and Range, western United States, and central Greece, and from the Miocene rift in the Gulf of Suez and has significant implications for our understanding of extensional basin development.

[3] Often overlooked, however, in the discussion of relay zones and extensional basin development are the dynamics of the geomorphic systems that are responsible for basin filling [*Bentham et al.*, 1991]. Mass transfer across a crustal-scale fault occurs via a series of fluvial catchments that efficiently parse the available footwall drainage area and feed sediment into a set of hanging wall fans. The precise

[1]Institute of Geology, Department of Earth Sciences, ETH Zürich, Zürich, Switzerland.
[2]Department of Geology, Tulane University, New Orleans, Louisiana, USA.
[3]Department of Earth Sciences and Engineering, Imperial College, London, UK.
[4]Department of Geology and Geophysics, University of Edinburgh, Edinburgh, UK.

0148-0227/03/2001JB001741$09.00

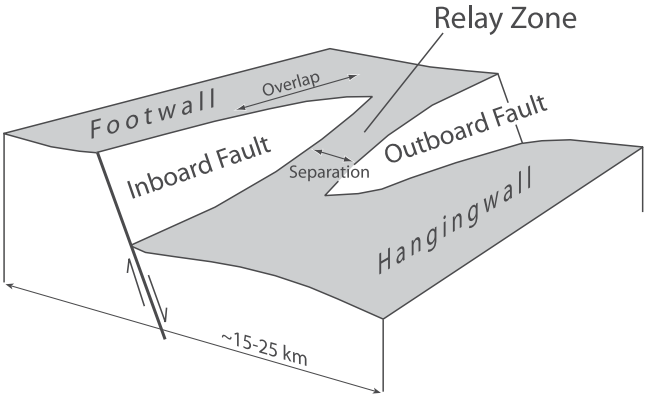

Figure 1. Perspective view of a soft-linked extensional relay zone, defining the terms used in this paper.

processes that operate in these catchment-fan systems vary with climate, fault slip rate, rock type, sediment supply, and proximity to base level. One reason why these processes have not been well studied in many extensional settings is that much of the work on relay zones has focused on older rifts, in which the catchments no longer exist [e.g., *Gupta et al.*, 1999; *Dawers and Underhill*, 2000; *McLeod et al.*, 2000]. The growing integration of research in tectonics and surface processes over the last decade allows us to approach this problem from a more holistic viewpoint.

[4] For example, it is increasingly clear that even simple extensional fault blocks are complex systems. Because of high spatial variability in footwall denudation, tectonic displacements cannot be used as simple proxies for paleo-footwall surface elevations, or vice versa [*Ellis et al.*, 1999]. Likewise, sediment discharge from catchments in extensional fault blocks is a function of a number of hillslope and channel processes and is difficult to predict simply based on tectonic displacements. In fact, changes in fault displacement rates may have surprising and counterintuitive effects on sediment supply [*Allen and Densmore*, 2000]. This stems from the fact that there are several timescales inherent in the catchment-fan systems, including (1) the time required to excavate the catchments and fully parse the available footwall drainage area [*Ellis et al.*, 1999] and (2) the time required for catchments to respond to changes in climatic or tectonic conditions [*Allen and Densmore*, 2000].

[5] In this paper we attempt to understand how the evolution of catchments and fans within extensional relay zones is affected by fault array growth. We first briefly discuss the evolution of fault arrays and the competing timescales of array growth and landscape response. Next, we present the results of numerical experiments that help to show how footwall landscapes develop in relay zones and how sediment is delivered from relay zones to adjacent basins. We drive these experiments with two very different tectonic boundary conditions, one in which the fault geometry is static during landscape evolution, the other in which the fault geometry varies continuously. We find that these two boundary conditions lead to very different landscape evolution pathways, with implications for footwall denudation patterns and sediment supply in the early stages of basin development. We also find that it is difficult to generate large relay zone catchment-fan systems in any of the experiments. We consider some physical reasons for this difficulty and illustrate these reasons with observations of relays along several active normal faults in the Basin and Range.

2. Fault Array Evolution

[6] It is now well established that many extensional faults evolve by the growth and mechanical linkage of individual segments [e.g., *Peacock and Sanderson*, 1991; *Anders and Schlische*, 1994; *Trudgill and Cartwright*, 1994; *Wu and Bruhn*, 1994; *Dawers and Anders*, 1995; *Cartwright et al.*, 1996; *Crider and Pollard*, 1998; *Gupta and Scholz*, 2000; *McLeod et al.*, 2000] and that fault evolution has a direct impact on the geometry and stratigraphy of adjacent extensional basins [*Leeder and Gawthorpe*, 1987; *Schlische*, 1991; *Gupta et al.*, 1998; *Cowie et al.*, 2000; *Dawers and Underhill*, 2000; *Gawthorpe and Leeder*, 2000].

[7] In the initial stages of fault array evolution, many faults tend to nucleate over a broad area, but with increasing strain, en echelon segments experience along-strike enhancement of stresses and thus deformation localizes on these segments [*Cowie*, 1998; *Gupta et al.*, 1998]. Meanwhile, the tips of other growing segments become essentially pinned, as regions of stress reduction around neighboring segments inhibit tip propagation [e.g., *Bürgmann et al.*, 1994; *Willemse et al.*, 1996; *Cowie*, 1998; *Gupta and Scholz*, 2000]. This establishment of en echelon geometry, with deformation localized onto a few major structures, means that segments must continue to accrue displacement with relatively little tip propagation; thus further deformation must be accommodated within evolving relay zones between overlapping segments (Figure 1).

[8] Studies of displacement variation across relay zones demonstrate that these zones are not regions of significant displacement deficit but rather are areas where total displacement is distributed across several fault strands [*Peacock and Sanderson*, 1991; *Trudgill and Cartwright*, 1994; *Dawers and Anders*, 1995; *Childs et al.*, 1995; *Cartwright et al.*, 1995, 1996; *Huggins et al.*, 1995; *Crider and Pollard*, 1998], such that the overall displacement on the fault system tends toward that expected for a single, isolated fault [*Dawers and Anders*, 1995; *Gupta and Scholz*, 2000]. Initially, ''soft-linked'' fault segments, connected by relatively unfaulted relay zones [*Walsh and Watterson*, 1991], will give way to ''hard-linked'' faults as the relay zones experience increased strain and are eventually breached by transfer faults.

3. Catchment-Fan Development in Relay Zones

[9] *Crossley* [1984] and *Leeder and Gawthorpe* [1987] both described field examples of large catchments located within low-relief relay zones between adjacent normal fault segments. *Leeder and Gawthorpe* [1987] went on to suggest that this might lead to large sediment discharges from these catchments, and the deposition of larger-than-normal fans within the adjacent hanging wall. This association has been developed and refined by a number of workers into what might be called the ''large-catchment'' model of relay zone geomorphology [e.g., *Gawthorpe and Hurst*, 1993; *Leeder and Jackson*, 1993; *Eliet and Gawthorpe*, 1995; *Gupta et*

al., 1999; *Gawthorpe and Leeder*, 2000; *Strecker et al.*, 2003], and has become almost axiomatic in studies of extensional basin development. It is thus important to understand the general applicability of this model and the constraints on relay zone catchment-fan development.

[10] The ideas behind the large-catchment model may be summarized as follows: areas between growing fault segments have relatively low topography through which any regional drainage, antecedent to the growing faults, can be funnelled. These areas may also collect drainage area from the back of the developing footwalls [e.g., *Leeder and Jackson*, 1993; *Strecker et al.*, 2003]. As the fault tips propagate toward one another and as fault segments interact and eventually link, the large catchments become increasingly confined within the relay zones, and bend to flow down the relay ramps between segments (Figure 1). Once the fault array becomes fully mechanically linked, the relay zones (whether breached or not) retain their large catchments, while catchments in the adjacent footwalls are typically much smaller [*Leeder and Jackson*, 1993; *Jackson and Leeder*, 1994]. Because discharge of water and sediment are functions of catchment area, the large relay zone catchments produce large-volume sedimentary fans in the hanging wall [*Leeder and Gawthorpe*, 1987; *Gawthorpe and Hurst*, 1993; *Leeder and Jackson*, 1993; *Gawthorpe and Leeder*, 2000].

[11] There is no doubt that catchments and fans in some relay zones do indeed evolve according to this model. However, there are several aspects of relay zone geomorphology that require more careful analysis in isolated fault blocks, that is, extensional settings in which the available catchment area is limited to the local fault footwall. Below, we consider these through the application of a numerical landscape evolution model. We focus on the development of catchment-fan systems in the face of two very different fault array growth scenarios: one in which array growth is rapid compared to the time required for catchment-fan system evolution, the other in which it is not. We specifically ignore the effects of regional drainage systems that predate the growing fault array. For simplicity, we also ignore the effects of climate change on catchment-fan evolution. This is partly justifiable in that climatic variations occur on short timescales ($\leq 10^5$ years) compared to the timescales inherent in fault array development or landscape evolution, and, unlike changes in fault behavior, climatic variations provoke a rapid response within the catchment-fan systems [e.g., *Allen and Densmore*, 2000].

4. Competing Timescales

[12] A central issue in understanding catchment development and sediment transport in relay zones is the interplay between two very different timescales: the timescale over which the fault array evolves, and the timescale over which the catchment-fan systems grow and respond to tectonic displacement. Consider two end-member scenarios. In the first, fault tips propagate rapidly, and the fault array achieves its final map-view geometry before accumulating much displacement and before significant denudation of the footwall can occur. Thus the footwall catchments develop within a tectonic displacement field characterized mainly by displacement accumulation rather than tip propagation. As described below, the low tectonically induced slopes and limited available drainage area within the relay zone in this scenario will militate against the development of large relay zone catchments. Importantly, in this scenario sediment transport and delivery to the basin are largely insensitive to the details of the fault growth process, because most sediment transport occurs after the overall along-strike fault architecture is determined.

[13] In the second scenario, fault segment growth is slow relative to catchment development and footwall denudation, so that the catchments must respond to a constantly changing tectonic displacement field both along and across strike. *Strecker et al.* [2003] explored this possibility and argued that such conditions lead to the focusing of footwall drainage through gaps between fault segments. As the faults propagate into en echelon geometries, this focusing through what are, in essence, inherited ''corridors'' will lead to large relay zone catchments, similar to the conceptual models described above [e.g., *Gawthorpe and Leeder*, 2000]. Whether or not this process occurs, we agree that catchments in this second scenario will evolve dynamically in a time-varying displacement field and will be strongly sensitive to the details of fault propagation. We expect that in such cases sediment discharge to the basin may vary dramatically in space and time because of drainage divide migration and increasing displacement rates on the faults that survive the competitive growth process [e.g., *Cowie*, 1998; *Gupta et al.*, 1998; *Cowie et al.*, 2000; *Gupta and Scholz*, 2000].

[14] These scenarios are analogous to the end-member cases of fault linkage described by *Cowie et al.* [2000]. In their case 1, linkage between fault segments occurred rapidly, leading to a long but under-displaced fault array [e.g., *Cartwright et al.*, 1995] and a broad, shallow hanging wall basin with only limited subbasin development. In contrast, case 2 involved fault interaction and displacement profile adjustment before physical linkage occurred [*Cowie et al.*, 2000], leading to persistent subbasins and a very different pattern of accommodation generation. Here, we extend those cases to include the development of the sediment transport systems.

[15] Unfortunately, field data on the relative timescales of fault linkage and footwall denudation are scarce and equivocal. A few studies have attempted to constrain tip propagation rates on individual fault segments. *Jackson and Leeder* [1994] used field observations and theoretical models to estimate that the tip of the Pearce segment of the Pleasant Valley fault in Nevada grew by 25 to 50 m per earthquake, which yields a tip propagation rate of $\sim$10 mm yr^{-1} given an earthquake recurrence interval of 10^3 to 10^4 years. *Morewood and Roberts* [1999] inferred a propagation rate of 12 to 16 mm yr^{-1} for the tip of the South Alkyonides fault in central Greece. Both estimates fall at the lower end of the range of propagation rates ($\sim$10 to 100 mm yr^{-1}) predicted by the geometrical model of *Cowie and Scholz* [1992a] for Basin and Range faults with lengths of $\sim$50 km. Other investigators have examined the timescales over which individual fault segments grow and link into arrays. *Morley* [1999] argued that basins along the East African Rift showed little evidence of changes in synrift fault geometry, implying that the fault arrays developed rapidly, before large volumes of sediment were deposited.

McLeod et al. [2000] showed that linkage of the >62 km long Strathspey-Brent-Statfjord fault array in the northern North Sea took 3 to 4 Myr after the onset of rifting. Working at one of the tip regions of the same array, *Dawers and Underhill* [2000] found an average rate of fault tip propagation over ~20 Myr of 0.25 to 0.5 mm yr^{-1}. They suggested that individual fault segments became incorporated into the array over timescales of several million years.

[16] Our understanding of the time required to develop a catchment-fan system, and transport significant amounts of sediment, is even poorer, and comes mostly from numerical modeling. *Ellis et al.* [1999] argued that Basin and Range-scale footwalls, i.e., blocks 10 to 15 km wide in the across-strike direction, with catchment lengths of 5 to 10 km - required $\sim 10^6$ years to achieve steady state relief, implying that this represents the timescale over which the catchment-fan systems become fully developed. *Allen and Densmore* [2000] found that, once established, these catchment-fan systems responded to changes in the tectonic displacement field much more rapidly, over timescales of ~50 kyr. A similar response time to changes in tectonic forcing over similar length scales was described by *Hardy and Gawthorpe* [2000]. It should be emphasized that these numbers are strongly model dependent. They do suggest, however, that complete reorganization of the footwall drainage system is unlikely if the fault array geometry becomes fully established in much less than $\sim 10^6$ years.

[17] The discrepancies in fault linkage timescales between different regions may be due to the fact that rift geometry, the initial fault nucleation pattern [e.g., *Cowie*, 1998; *Cowie et al.*, 2000], and strain rate may all influence fault propagation rates; thus generalization of results between rifts may not be possible. In the absence of any clear agreement on how fault propagation and landscape response timescales might interact, we use a numerical landscape evolution model to evaluate the behavior of the two end-member scenarios described above. We show that changes in the timescale of fault growth lead to very different landscape evolution pathways, and we point out the difficulty of generating large relay zone catchment-fan systems.

5. Landscape Evolution Model

[18] The landscape evolution model Zscape was developed specifically to understand the topographic development of Basin and Range-scale fault-bounded blocks, and has been used to explore the importance of bedrock landslides in montane areas [*Densmore et al.*, 1998], the generation of triangular facets and other landforms associated with normal faults [*Ellis et al.*, 1999], and the influence of tectonic and climatic conditions on catchment denudation and sediment flux in simple fault blocks [*Allen and Densmore*, 2000].

[19] Here, we extend the results of *Allen and Densmore* [2000] by considering fault geometries that incorporate relay zones between two en echelon fault segments. A brief description of Zscape is included here, but full details are given in the work of *Densmore et al.* [1998] and *Allen and Densmore* [2000]. The model operates on a two-dimensional finite difference grid, and each model cell is associated with a value of both surface elevation and bedrock surface elevation. The model topography at the beginning of each experiment is a planar sheet, gently sloping toward the future hanging wall, with randomly distributed perturbations of up to one meter that introduce variation into the initial drainage pattern. Deformation of the bedrock and landscape surfaces is accomplished by applying a three-dimensional tectonic displacement field generated by an elastic half-space model [*Gomberg and Ellis*, 1994]. Applications of the displacement field occur at a specified recurrence interval, left constant in these experiments, and are analogous to coseismic deformation during an earthquake; we neglect post- and interseismic deformation. The resulting topography is acted upon by a series of algorithms that simulate regolith production, diffusive hillslope sediment transport, bedrock landsliding, alluvial sediment transport, and fluvial incision into bedrock [*Densmore et al.*, 1998]. Bedrock lithology and erodibility are assumed to be uniform throughout the model space. Model dimensions in all experiments are 15 × 15 km, individual cells are 100 by 100 m, and the time step is 10 years. The model precipitation rate is held constant and uniform at 0.5 m yr^{-1}. During each experiment, the model is run until the footwalls reach a steady state catchment relief. Beyond that stage, the details of the topography will vary, but the maximum relief and hypsometry of the footwall remain approximately constant [*Ellis et al.*, 1999; *Willett and Brandon*, 2002].

[20] As with any numerical landscape evolution model, there are several parameters in the geomorphic rule set whose values are not physically meaningful and difficult to constrain [see *Densmore et al.*, 1998]. For simplicity, we leave these parameters unchanged during the numerical experiments described here. Instead, we evaluate the robustness of the results by running sensitivity analyses in which we vary only the maximum fault slip rate and the model precipitation rate. The fault slip rate dictates the rate of base level fall and accommodation generation in the model space, while the model precipitation rate is proportional to the rates of fluvial sediment transport and bedrock channel incision. Thus these two parameters allow us to vary the relative importance of tectonic and geomorphic material fluxes within the model space.

6. Numerical Experiments

[21] We show the results of two experiments that differ only in the tectonic displacement fields used to generate topography. In experiment 1, a single displacement field is used throughout the experiment and includes two separate, soft-linked en echelon fault segments, both 40 km long, 15 km wide in the down-dip direction, and dipping 45° in the same direction (Figure 2). Separation between the segments is 5 km and overlap is 8 km, similar to observed en echelon relay zones in the Basin and Range. The faults are driven by a pure shear extensional displacement gradient field, such that the maximum slip per event on each fault is ~3 m. The recurrence interval between applications of the displacement field is set to 3300 years to yield a long-term maximum slip rate of about 1 mm yr^{-1}. The fault tips are pinned throughout the model run; this simulates a situation in which fault tip propagation and segment interaction occur very rapidly, resulting in the establishment of a soft-linked geometry before the topography can respond. The maxi-

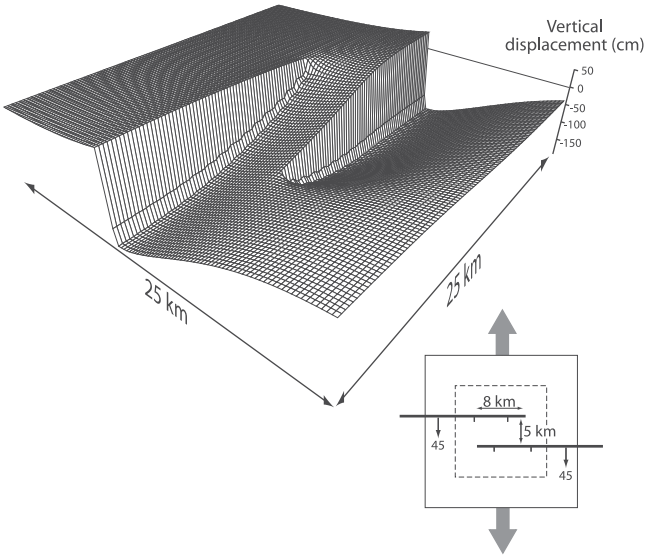

Figure 2. Perspective view of the vertical component of the static, en echelon tectonic displacement field used in experiment 1. Faults dip 45° and are 40 km long. Displacement field corresponds to a single coseismic event, and is applied to the model landscape at a specified recurrence interval of 3300 years, yielding a long-term maximum slip rate of 1 mm yr^{-1}. Inset shows the map-view fault geometry and the orientation of the pure shear displacement gradient tensor used to drive deformation (large arrows). Dashed box in inset shows the 15 × 15 km landscape evolution model space used in the numerical experiments.

mum displacement on each fault at the end of the experiment is ~5 km. Note that, because the fault tips are pinned, the ratio of maximum displacement to segment length (D/L ratio) increases during the experiment, to a maximum value of 0.13 after 5000 kyr of model run time. This evolution of segment D/L ratios is comparable to field and numerical studies of en echelon fault arrays, which show that the D/L ratio for individual interacting segments may increase to a value 3 to 10 times that of a more isolated fault [*Dawers and Anders*, 1995; *Willemse et al.*, 1996; *Schlische et al.*, 1996; *Gupta and Scholz*, 2000]. The 15 × 15 km model space is centered within a 25 × 25 km displacement field in order to prevent edge effects and to allow for three-dimensional displacements of the model grid (Figure 2). Because the grid points undergo horizontal as well as vertical deformation, the topography is resampled using bilinear interpolation once the maximum cumulative grid displacement has reached 1/4 of the 100 m grid spacing. This resampling has no visible effect on the drainage pattern evolution.

[22] In experiment 2, we again employ two faults dipping 45°, but we allow the fault tips to propagate toward one another during the initial part of the model run (Figure 3). The faults begin as short (16 km) segments with 5 km separation and 16 km underlap, so that initially they behave as isolated faults within the elastic half-space. The fault tips propagate in 1 km increments after every 20 coseismic events; because the recurrence interval is 3300 years, this corresponds to a propagation rate of 15 mm yr^{-1}. Propagation ceases after 800 kyr of model run time, once the adjacent fault tips have propagated 12 km; at this point the faults are 40 km long and overlap by 8 km, the same geometry as that used in experiment 1. For the remaining 5200 kyr of experiment 2 the displacement field remains static and is identical to that used in experiment 1.

[23] For simplicity, the tip propagation rate is held constant throughout the model run, despite observational evidence and theoretical arguments that the rate probably decreases as the tips approach one another [e.g., *Gupta and Scholz*, 2000]. In addition, we do not explicitly scale the displacement by an expected D/L ratio, nor do we specify a particular threshold D/L ratio at which the fault tip propagates. However, during the propagation phase of the experiment the D/L ratios of the faults vary between 0.003 and 0.02, within the range of ratios observed in isolated faults (0.001 to 0.06 [e.g., *Cowie and Scholz*, 1992b; *Dawers et al.*, 1993; *Schlische et al.*, 1996]). Finally, it should be noted that the elastic half-space fault model produces an approximately elliptical distribution of slip along each fault. Displacement thus decreases rapidly toward the fault tips, which contrasts with the linear displacement gradient observed and predicted by *Cowie and Shipton* [1998].

[24] It is important to emphasize that the displacement fields used in these experiments are extremely simplified, both in geometry and in temporal evolution, compared to real relay zones. For example, we have not explored the sensitivity of our topographic results to different fault tip displacement gradient patterns [*Cowie and Shipton*, 1998], nor have we evaluated the effects of varying the size of the increment by which the fault tips propagate, although these variables affect the displacement field and are thus likely to have some effects on the topographic evolution of the footwall. Our intention is not to simulate precisely the growth of a set of en echelon faults, nor to reproduce

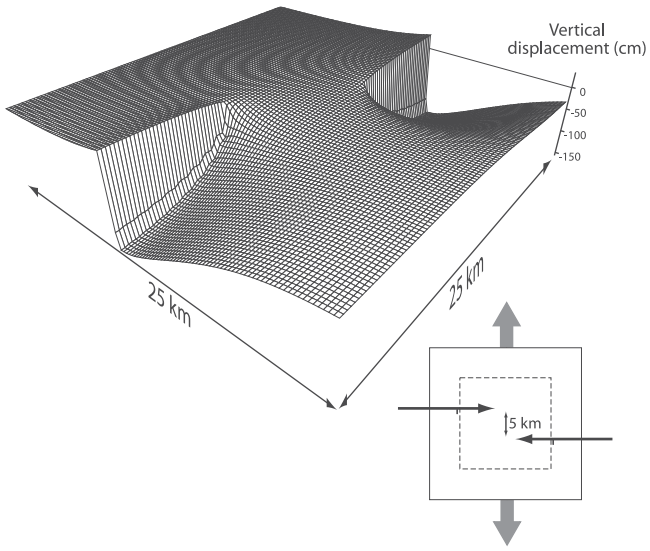

Figure 3. Perspective view of the vertical component of the propagating tectonic displacement field used in experiment 2. At this point, after 550 kyr of model run time, the faults have propagated 8 km toward each other and are 32 km long. Faults dip 45° as in Figure 2.

the exact topography of a particular relay zone. Instead, our goal is to compare catchment-fan systems developed in the face of two very different tectonic boundary conditions: one in which the fault geometry is static during landscape evolution, the other in which the fault geometry varies continuously, albeit in relatively large increments.

7. Experimental Results

7.1. Experiment 1: Static Fault Geometry

[25] The faults in experiment 1 maintain the same overlapping en echelon geometry throughout the experiment, and no fault tip propagation is allowed. After 800 kyr of model run time, rapid base level fall along the inboard and outboard faults (see Figure 1 for terminology) has caused catchment incision and fan progradation, especially near the edges of the model space where the rate of base level fall is highest (Figure 4a). The relay zone is deformed by displacement on both faults, such that the overall topographic slope of the relay is fault-parallel with a slight tilt toward the inboard fault. This slope, coupled with the increase in displacement rate along the inboard fault away from the fault tip, produces a strongly axial relay zone drainage. Across most of the relay zone, the drainage divide between catchments flowing toward the inboard and outboard hanging walls is approximately parallel to the strike of the faults, and is located quite close to the outboard fault (Figure 4a). Thus, in the initial stages, most of the water and sediment derived from the relay zone are transported axially into the inboard hanging wall.

[26] After 3000 kyr, the model is approximately halfway through the time required to reach a steady state footwall relief (Figure 4b). At this stage, progradation of sediment onto the relay ramp has modified the topographic surface slope in the relay zone, so that it is more uniformly fault-parallel. This progradation also allows the relay zone drainage to flow around the tip of the outboard fault, causing migration of the drainage divide. A secondary drainage divide exists between the relay zone drainage, which flows around the outboard fault tip, and the catchments that directly drain the outboard footwall. Catchments in the outboard footwall experience a higher rate of base level

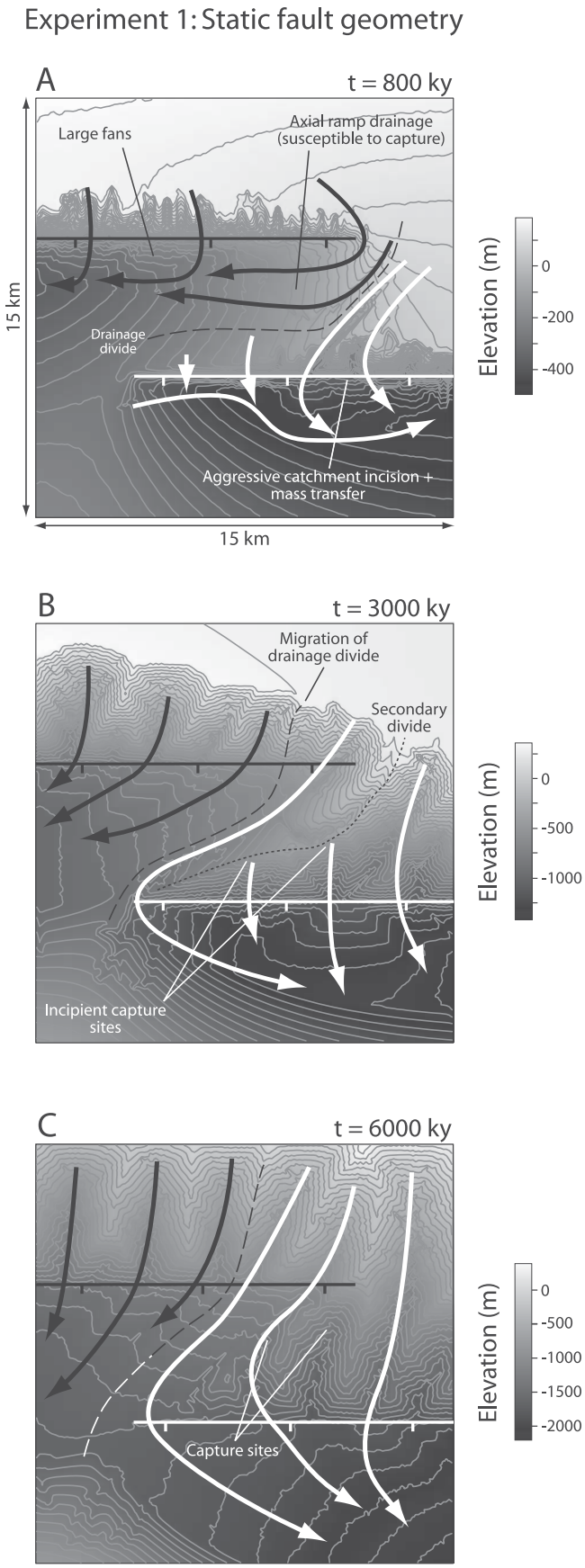

Figure 4. (opposite) Model topography from experiment 1, in which soft-linked fault geometry is established at beginning of experiment and fault tips remain pinned through the run. Topography shown by greyscale and contour lines. Thick straight lines show surface traces of the faults, with ticks on the downthrown blocks. Heavy arrows show generalized drainage directions. Dashed line is drainage divide between catchments draining toward inboard and outboard hanging walls. A, topography after 800 kyr of model run time. Contour interval 20 m. Note axially directed, fault-parallel relay zone drainage. B, topography after 3000 kyr. Contour interval 50 m. Note migration of drainage divide through fan propagation in the relay zone, and incipient destruction of secondary drainage divide in outboard footwall (dotted line). C, topography after 6000 kyr, with steady state footwall relief. Contour interval 75 m. Note elimination of secondary divide and relict capture sites.

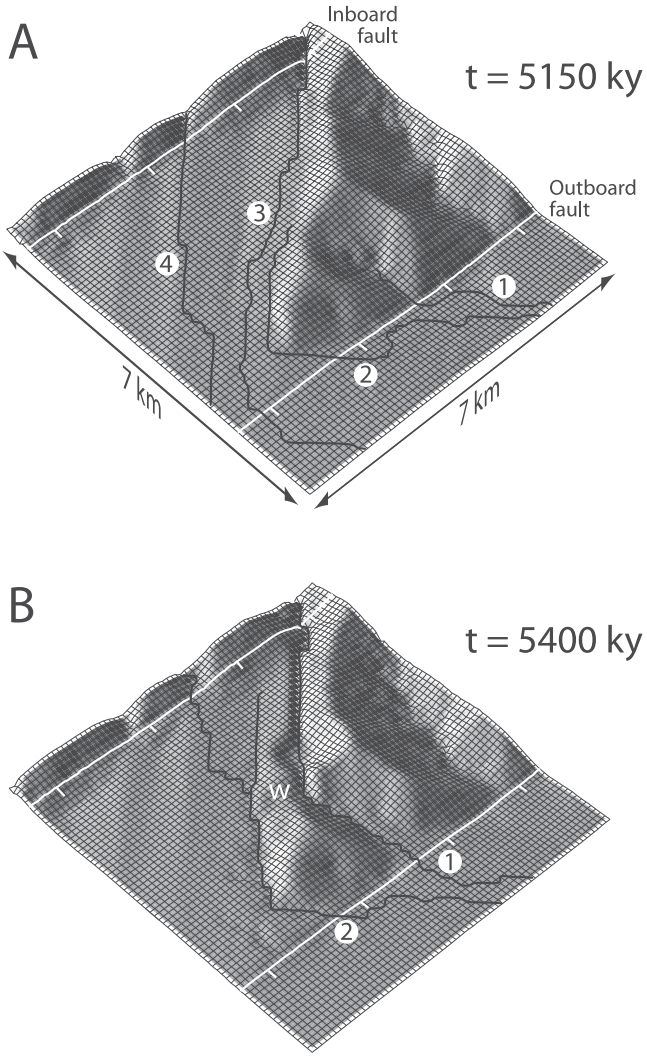

Figure 5. Shaded-relief perspective views of the topography before and after a capture event during experiment 1. A, topography from a 7 × 7 km portion of the relay zone at 5150 kyr, before the capture event. Numbers 1–4 denote individual rivers. B, the same area at 5400 kyr, after the capture event. Headward incision of catchment 1 has first captured catchment 3; subsequently, incision of catchment 2 has captured catchment 4. White lines show faults, with ticks on the downthrown blocks. w, wind gap.

fall than catchments draining the relay zone and thus are able to rapidly incise headward into the relay. This incision leads to two major capture events between 3000 and 6000 kyr (Figures 4b and 4c). In each event, water and sediment that formerly flowed down the ramp and around the outboard fault tip are abruptly rerouted across the outboard footwall and into the growing fans adjacent to the outboard fault (Figure 5).

[27] After 6000 kyr, the experimental topography has reached a steady state footwall relief (Figure 4c). The main drainage divide between inboard and outboard hanging walls has continued to shift over the final 3000 kyr of the experiment due to progradation of thin fans across the relay zone. The secondary drainage divide has been completely destroyed by capture events, and the drainage pattern has now reached a quasi-stable state. If the model run is continued, the individual catchment areas vary, but the gross drainage pattern and drainage divide position remain unchanged [e.g., *Ellis et al.*, 1999].

[28] It is important to note that no abnormally large relay zone catchment develops during experiment 1. Likewise, the spatial pattern of sediment thickness at the end of experiment 1 shows that there is no correspondingly large relay zone fan (Figure 6). In a series of experiments designed to test whether this is a robust outcome of experiment 1, we observe this same basic drainage pattern for a range of maximum fault slip rates (0.5 to 2.0 mm yr^{-1}), and for a range of uniform, constant model precipitation rates (0.5 to 2.0 m yr^{-1}).

7.2. Experiment 2: Propagating Fault Geometry

[29] In experiment 2, the fault tips are initially located at the edges of the model space and propagate toward one another at a rate of 15 mm yr^{-1}. After 800 kyr, the faults reach the same en echelon geometry as that used in experiment 1, and the geometry then remains constant for the remainder of the experiment. The topography after 800 kyr of model run time is very different from that of experiment 1 (Figure 7a). The propagation of the tips into the model space ensures that, at any one point, the total displacements after 800 kyr are less than in experiment 1, and so there is less footwall incision and fan progradation. The time-vary-

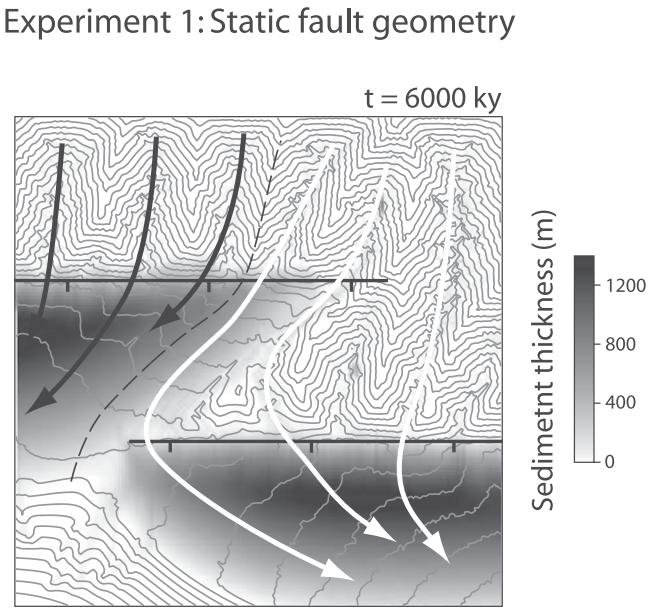

Figure 6. Sediment thickness at the end of experiment 1, after 6000 kyr of model run time. Dark colors indicate high sediment thicknesses. Contours show surface topography for reference; contour interval 75 m. Black lines show surface traces of the faults. Arrows show generalized drainage directions. Dashed black line is drainage divide between catchments draining toward inboard and outboard hanging walls. Note that very little sediment is preserved in the relay zone or in the adjacent hanging wall. Most deposition occurs away from the relay, where fault displacement rates, and rates of accommodation generation, are highest.

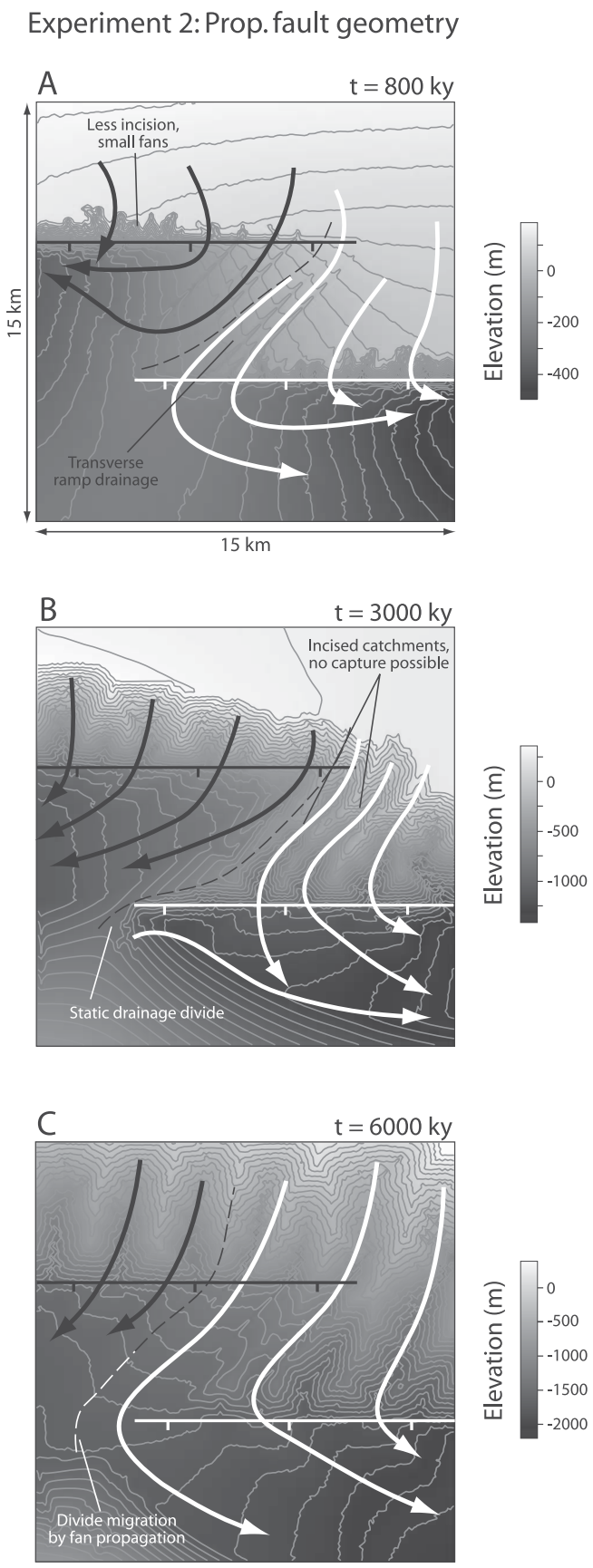

ing nature of the displacement field generates a relay zone in which the topographic slope is directed outward, toward the hanging wall. Thus, in contrast to experiment 1, the relay zone drainage in experiment 2 is dominantly transverse, rather than axial. The drainage divide between catchments flowing to the inboard and outboard footwalls extends between the fault tips, bisecting the relay zone.

[30] After 800 kyr, the tectonic displacement field used in experiment 2 is soft-linked, identical to that used in experiment 1. Thus, after 3000 kyr, topography has evolved in response to this shared displacement field for more than 2/3 of the total run time. Despite this, at 3000 kyr there are still significant differences in drainage pattern between the experiments. Figure 7b shows that the gross drainage pattern in experiment 2 is largely unchanged between 800 and 3000 kyr. The drainage divide position remains essentially static and is formed by a ridge that separates two relatively equally incised catchments, implying that capture of relay zone drainage is unlikely to occur.

[31] The landscape in experiment 2 reaches steady state footwall relief after approximately 6000 kyr. By this point, the topography looks very similar to that from Experiment 1 (Figure 7c). This is not surprising, as the displacement field is the same in all but the first 800 kyr of the experiments. Once again, no large relay zone catchment-fan system has developed. The key difference between the results of experiments 1 and 2 lies not in the final topography, but in the evolution of the landscape toward that final state. In experiment 2, the final 3000 kyr of model run time is characterized by slow migration of the drainage divide toward the inboard hanging wall as thin fans prograde from the relay zone and the inboard footwall. Overall, the gross catchment pattern remains the same throughout this interval. Unlike experiment 1, no major drainage reorganizations or capture events occur, and there are no sudden shifts in the loci or rate of sediment delivery to the outboard hanging wall. Figure 8 shows the mean fan deposit thickness in the outboard hanging wall as a function of time in both experiments. Fans are initially slightly thicker, on average, in experiment 1 because of the more rapid accumulation of displacement in the initial 800 kyr, but this difference disappears by 1500 kyr and the mean fan thicknesses are approximately equal until ~3500 kyr. After this point, the capture events during experiment 1 cause an increase in the rate of sediment accumulation in the outboard fan, relative

Figure 7. (opposite) Model topography from experiment 2, in which fault tips propagate at 15 mm yr^{-1} for the first 800 kyr of the experiment until the faults reach the soft-linked fault geometry used in Experiment 1. After 800 kyr the fault tips remained pinned, as in experiment 1. Symbols as in Figure 4. (a) Topography after 800 kyr of model run time. Contour interval 20 m. Note transverse, fault-normal component of relay zone drainage. (b) Topography after 3000 kyr. Contour interval 50 m. Drainage divide remains static, and catchments in relay zone and outboard footwall are equally incised, making capture unlikely. (c) Topography after 6000 ky, with steady state footwall relief. Contour interval 75 m. Note lack of change in gross drainage pattern throughout experiment, and similarity of final topography with that of Figure 4c.

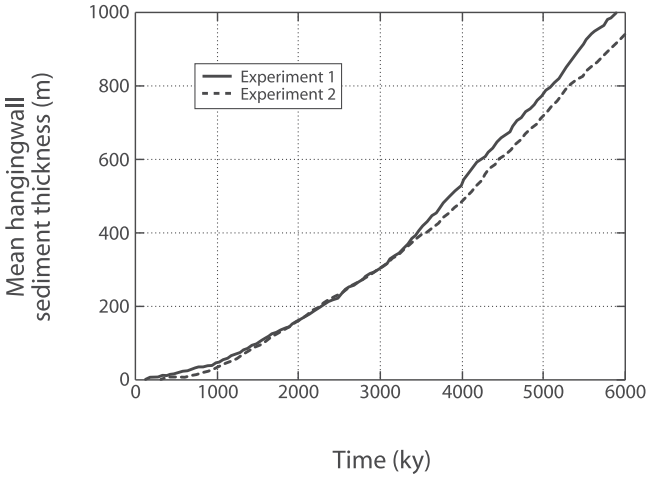

Figure 8. Mean sediment thickness in the outboard hanging wall as a function of time during experiments 1 and 2. Hanging wall fans are slightly thicker in experiment 1 before 1500 kyr because of more rapid base level fall relative to experiment 2 during first 800 kyr. Mean fan thickness increases more rapidly in experiment 1 after 3500 kyr due to capture events in outboard fault footwall.

to experiment 2 (Figure 8). Thus the loci of sediment delivery to the outboard hanging wall, and the rate at which the fans accumulate, change substantially due to these capture events, despite the fact that the fault geometry, slip rate, and climatic conditions have all remained constant throughout the run. Again, these experimental results are insensitive to different values of the maximum fault slip rate (0.5 to 2.0 mm yr^{-1}) and the model precipitation rate (0.5 to 2 m yr^{-1}).

[32] In summary, three points are worth noting. First, the rate of fault tip propagation (and thus the timescale over which the fault array grows) has a powerful influence on the evolution of the model footwall topography in the first few million years of landscape evolution. In particular, the presence or absence of relay zone drainage capture by headward incision of catchments in the outboard footwall appears to be a key difference between the experiments, and may represent a diagnostic tool for distinguishing between these scenarios in real field examples. Second, despite these differences in the initial stages, the catchment pattern and footwall topography in both experiments eventually converge to a single overall form in the face of the same tectonic displacement field. This suggests that footwall topography may be of limited use in reconstructing fault array evolution beyond a particular time window. Finally, neither experiment produces either a large relay zone catchment or a large associated fan. This result is directly contrary to the large-catchment model of relay zone geomorphology described in the sections above, a discrepancy that we address in the following section.

8. Physical Constraints and Comparisons With Basin and Range Relay Zones

[33] Because large relay zone catchment-fan systems do not form in the numerical experiments, we cannot specify the conditions needed to generate them in isolated fault blocks. However, we can use the results of the numerical experiments to identify several important physical constraints on catchment-fan system growth in relay zones. We emphasize again that we do not seek to understand all controls on the geomorphic evolution of relay zones, nor do we attempt to recreate the evolution of one particular relay zone. Instead, we illustrate these general considerations with several examples of relay zones in the Basin and Range province in which these constraints appear to have affected either catchment size or evolution.

8.1. Geometric Constraints on Catchment Area

[34] Development of large catchments in relay zones requires, first of all, that sufficient drainage area is available. In the presence of active fault slip and base level fall, footwall drainage area is a scarce resource that is competitively divided between neighboring catchments. Unless a relay zone catchment is antecedent, thus tapping a reservoir of drainage area outside of the local fault footwall, its growth will be highly constrained both by catchments in the adjacent footwalls and by catchments draining the other side of the fault block. These constraints typically result, in the absence of antecedent drainage or lithological variations, in catchments of very similar size along strike [e.g., *Wallace*, 1989b]. This behavior is shown by both experiments 1 and 2 (e.g., Figures 4c and 7c).

8.2. Catchment Growth

[35] Assuming that sufficient drainage area is available, relay zone catchment growth then depends on the rate at which the catchment can enlarge itself at the expense of its neighbors. *Densmore et al.* [1998] suggested that the rate-limiting process for headward catchment enlargement in Basin and Range-scale fault blocks undergoing active deformation and base level fall was the rate of channel incision into bedrock, and that hillslope denudation by bedrock landsliding was highly efficient at keeping pace with catchment incision. The rate of fluvial incision into bedrock is itself dependent on a number of factors [e.g., *Sklar and Dietrich*, 1998; *Hancock et al.*, 1998; *Whipple et al.*, 2000] but is commonly assumed to be a power law function of catchment area and channel slope (the so-called stream power incision rule) [e.g., *Whipple and Tucker*, 1999]:

$$\frac{\partial z}{\partial t} = kA^m S^n \tag{1}$$

where $\partial z/\partial t$ is bedrock incision rate (m yr^{-1}), A is catchment area (m^2), S is channel slope (dimensionless), m and n are positive exponents that depend on catchment and channel geometry, and k is an empirical constant that depends on lithology and climate. Various versions of equation (1) exist; the rule used in Zscape, for example, includes a threshold area-slope product below which sediment transport and bedrock incision do not take place [*Densmore et al.*, 1998]. These general formulations are simplifications of the actual physics that underlie bedrock river incision but are somewhat consistent with both empirical evidence and theoretical arguments. All formula-

tions, however, include an explicit relationship between channel slope and bedrock incision rate. By definition, fault displacement rates and tectonically induced fault-perpendicular slopes will be lower within relay zones than along adjacent footwalls, at least until significant mechanical interaction or full linkage of the fault array is achieved [e.g., *Gupta and Scholz*, 2000]. Thus we expect that relay zone catchments, all else being equal, should be relatively less capable of fluvial incision and headward enlargement than catchments farther along both the inboard and outboard faults, placing them at a disadvantage in the competition for footwall drainage area. This is clearly shown by the pattern of catchment-averaged erosion rates (which are limited by the rate of bedrock incision [*Densmore et al.*, 1998]) at the conclusion of experiment 1, which are lowest for the relay zone catchments and adjacent to the fault tips (Figure 9a).

[36] A likely example of this behavior occurs in Cache Valley, Utah, which lies in a relay zone between two active normal faults, the Collinston and Brigham City segments of the Wasatch fault to the west, and the East Cache fault zone [*McCalpin*, 1994] to the east (Figure 10). Maximum relief is 1500 m over a distance of 5 km (yielding a slope of $\sim$0.30 m m^{-1}) on the Wasatch fault footwall, and 1630 m over a distance of 11.5 km (slope of 0.14 m m^{-1}) on the East Cache fault footwall. In contrast, catchments in the relay zone have a maximum relief of 1300 m over a distance of 15.5 km (slope of 0.084 m m^{-1}). Catchment size in the Wasatch fault footwall is limited by base level fall and catchment development along the West Cache fault zone. The relay zone catchments, while larger than those in the Wasatch footwall, are not the largest in the area. In fact, the largest catchments are located in the footwall of the East Cache fault zone, where relief and tectonically induced slopes are high and drainage area is relatively unconstrained.

[37] An important corollary of this relationship between fault displacement rates, slopes, and headward enlargement is that catchments in the outboard footwall should, in some cases, be capable of incising headward rapidly enough to capture a large part of the relay zone drainage area and divert it into the outboard hanging wall, as was observed in experiment 1. This will result not only in decreased relay zone catchment size but also in decreased sediment discharge from the relay zone, as sediment bypasses the relay and is delivered directly to the outboard hanging wall.

[38] Capture of relay zone catchments is observed in several relay zones in the Basin and Range, most notably in the relay between the Blue Dome and Nicholia segments of the Beaverhead fault in south central Idaho (Figure 11 [*Anders and Schlische*, 1994]). Here, relay zone catchments once flowed down the ramp between the inboard and outboard faults. Incision of two catchments into the outboard footwall has progressively captured much of the relay zone drainage area (Figure 11). The resulting morphology is very similar to that developed by the series of capture events in experiment 1 (Figures 4c and 5). Again, none of the catchments within the Blue Dome relay zone are significantly larger than those in either of the adjacent footwalls (Figure 11). Thus, even if large relay zone catchments are able to develop initially, they will be vulnerable to capture by smaller, more aggressive catchments in the outboard

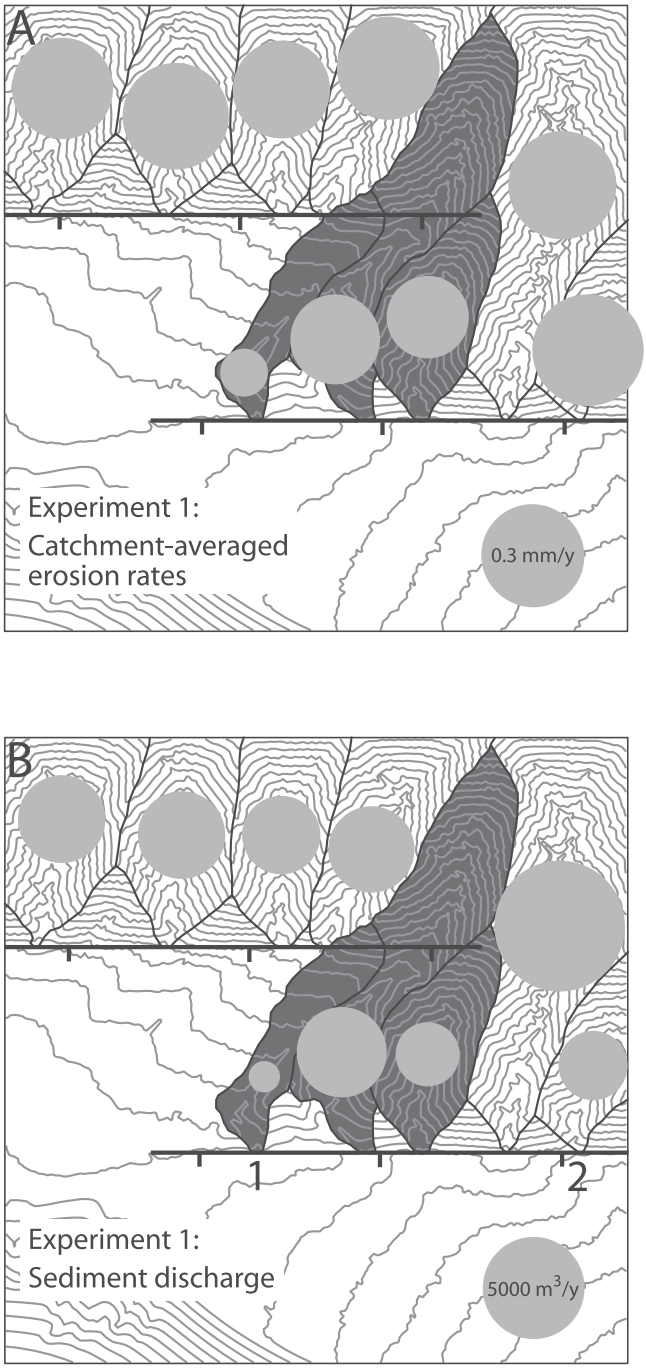

Figure 9. (a) Mean catchment-averaged erosion rate (mm yr^{-1}) at the end of experiment 1. Areas of circles are proportional to mean erosion rate. Reference circle represents 0.3 mm yr^{-1}. Contours show surface topography for reference; contour interval 75 m. Thick black lines show surface traces of the faults. Thin black lines show the footwall catchment boundaries. Relay zone catchments are shaded. (b) Sediment discharge at the end of experiment 1. Areas of circles are proportional to sediment discharge. Reference circle represents 5000 m^3 yr^{-1}. Note that relay zone catchments have relatively low erosion rates and discharge. Catchments 1 and 2 are comparably sized (6.97 and 6.28 km^2, respectively), but their different positions along the outboard fault lead to very different sediment discharge values. See text for discussion.

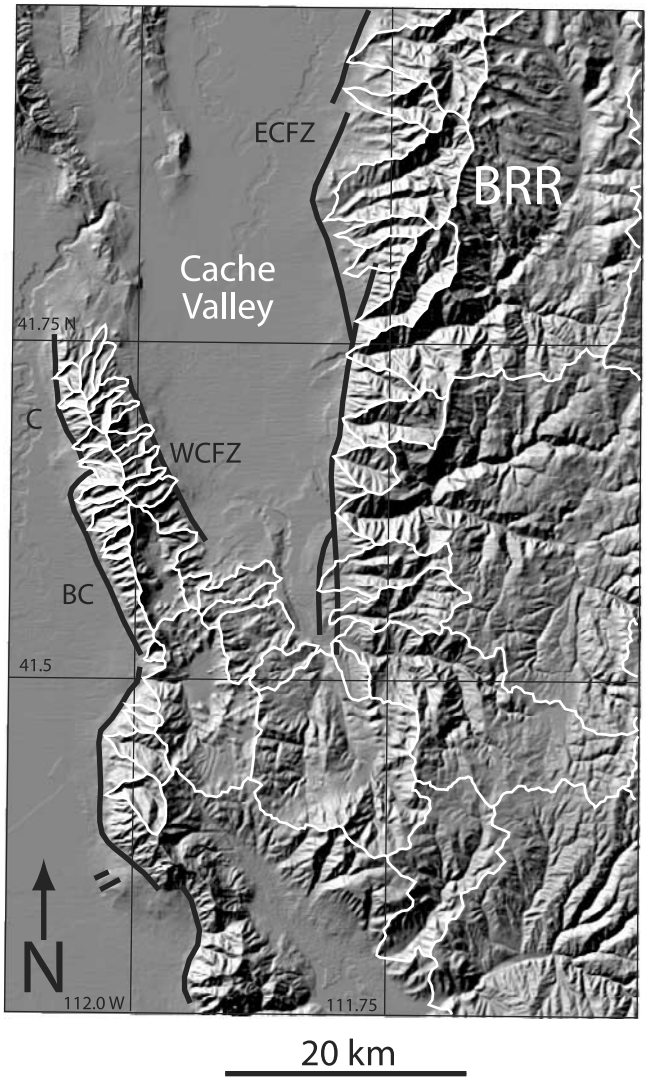

Figure 10. Shaded-relief image of topography from Cache Valley, Utah. Topography is derived from U.S. Geological Survey National Elevation Dataset data with 30 m resolution. Active faults are shown by black lines. The outboard footwall is bounded by the Collinston (C) and Brigham City (BC) segments of the Wasatch fault zone, and by the West Cache fault zone (WCFZ). The inboard footwall is bounded by the East Cache fault zone (ECFZ). White lines show the boundaries of the footwall catchments. Note that the largest catchments are located in the steep, high-relief inboard footwall. BRR, Bear River Range.

footwall whose headward incision is driven directly by rapid fault displacement and base level fall.

8.3. Sediment Discharge

[39] As far as we are aware, there are no direct measurements of sediment discharge or sediment flux that allow comparison between catchments in relay zones and on adjacent footwalls. The paucity of reliable long-term sediment discharge measurements from fault blocks in general means that sediment discharge is commonly assumed to be directly proportional to catchment area [e.g., *Gawthorpe and Hurst*, 1993; *Leeder and Jackson*, 1993; *Eliet and Gawthorpe*, 1995]. The relationship between equilibrium sediment discharge from a footwall catchment at steady state is typically assumed to be [e.g., *Whipple and Trayler*, 1996]:

$$Q_s = U_r(1 - \lambda_r)A \tag{2}$$

where Q_s is steady state sediment discharge ($m^3\ yr^{-1}$), U_r is a spatially uniform rock uplift rate ($m\ yr^{-1}$), A is catchment area (m^2), and λ_r is rock porosity.

[40] Even along geometrically simple normal faults with uniform footwall lithology, the controls on catchment sediment discharge are likely to be more complex than predicted by equation (2), and in particular must be highly spatially nonuniform. The underlying reasons for this are that fault displacement rates decrease both along strike (away from the center of a fault segment) and across strike (away from

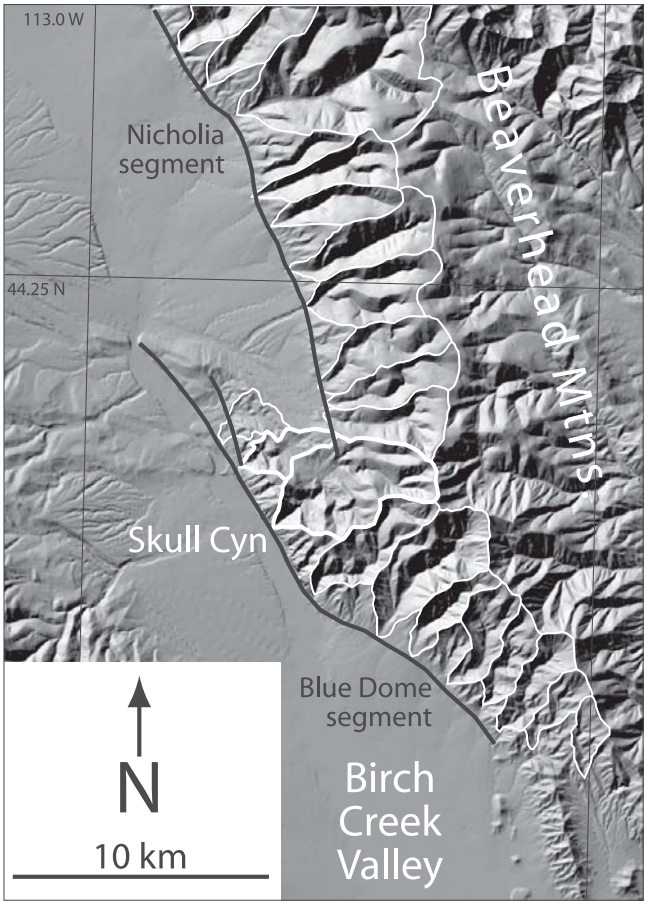

Figure 11. Shaded-relief image of topography near Blue Dome, Idaho. The outboard footwall is bounded by the Blue Dome segment of the Beaverhead fault, while the inboard footwall is bounded by the Nicholia segment. Active faults are shown by thick black lines. White lines show the boundaries of the footwall catchments. Note that Skull Canyon and a smaller, unnamed catchment to the north (thick white lines) have captured some of the relay zone drainage area and rerouted it into lower Birch Creek Valley. The largest footwall catchment is located away from the relay zone, in the steep, high-relief inboard footwall, at the top of the figure.

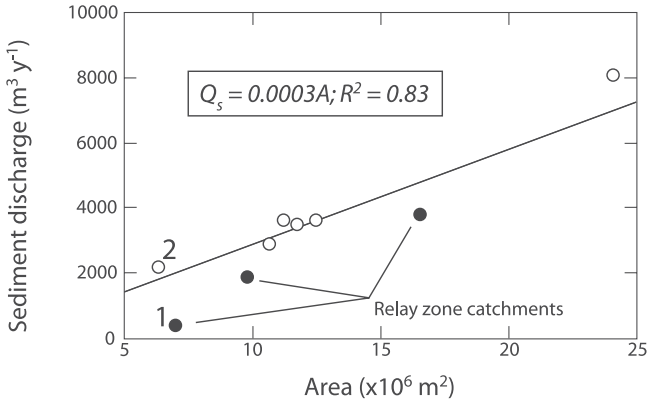

Figure 12. Sediment discharge from the catchments in Experiment 1 as a function of drainage area. Solid symbols show the three catchments in the relay zone. Catchment 1 is located at the tip of the outboard fault, in the relay zone, while catchment 2 is located on the outboard fault at the edge of the model space (see Figure 9b for locations). The solid line shows the best-fit linear regression line. Note that the regression overpredicts sediment flux from the relay zone catchments by up to a factor of 4, due to their low tectonic displacement rates.

the fault trace), and that footwall catchments are subjected to displacements in three dimensions, rather than simply to vertical rock uplift. Geologic and geodetic data along active normal faults consistently show that displacements are greatest at or near the fault trace, and decrease with distance away from the fault [*Stein et al.*, 1988; *Anders et al.*, 1993]. Thus different parts of each catchment experience different rock uplift rates relative to some downstream base level, even in steady state. *Densmore et al.* [1998] used this observation to argue that, in steady state, rates of hillslope denudation by bedrock landsliding, and fluvial bedrock incision rates, must increase from the headwaters of fault block catchments toward the mountain front. This implies that, for example, parts of a catchment close to the fault will produce higher sediment fluxes, or discharges per unit area, than those in the catchment headwaters.

[41] The results of experiment 1 agree with this expectation. Figure 9b shows sediment discharge from each catchment at the end of the experiment, once the footwall had reached a steady state relief. There is a clear positive correlation between catchment area and sediment discharge (Figure 12), in line with the simple assumptions behind equation (2). However, superimposed on this correlation is a second-order effect that derives from the rate of base level fall experienced by each catchment and the position of the catchment with respect to the loci of maximum rock uplift along each fault. Discharge values for catchments in the relay zone are overpredicted by the area-discharge relationship in equation (2), while values for catchments outside the relay zone are underpredicted (Figure 12). For example, catchment 2 (Figures 9b and 12) is the smallest catchment on the model space; yet it has the highest sediment flux and its sediment discharge is larger than that of two of the three relay zone catchments. This is simply due to its location close to the midpoint of one of the faults and the fact that its drainage area is concentrated in the zone of high displacement rates close to the fault. In contrast, catchment 1, which is 11% larger than catchment 2, experiences low displacement rates near the tip of the outboard fault and drains predominantly lower slopes due to the combined displacement on both faults. These factors result in extremely low sediment discharge values (Figure 12).

[42] The slope of 0.3 mm yr^{-1} in the area-discharge relationship in Figure 12 is effectively a spatially averaged catchment denudation rate, or alternatively a spatially averaged rock uplift rate if the footwall is truly in steady state. Recall that the slope of the line in equation (2) is controlled by the spatially uniform rock uplift rate relative to some base level. The relative slip rate across each model fault varies from 1.0 mm yr^{-1} at the edge of the model space to 0 at the fault tip, with a mean of 0.6 mm yr^{-1}. However, in reality, catchments incise not in response to the relative slip rate on the fault but to the rate of base level fall, which is controlled here by the rate at which the elevation of the edge of the model space changes relative to the footwall part of the catchment. Deposition in the hanging wall basin offsets some of the tectonic subsidence relative to the footwall. Thus, even in steady state, the relationship between fault slip rate and sediment flux in these catchments is not straightforward.

[43] The spatial position of a catchment relative to the fault is thus important in setting the sediment discharge. A small catchment whose drainage area is concentrated near the fault, in the zone of high rock uplift rates, may have a higher sediment flux, and perhaps even a higher sediment discharge, than a larger catchment whose drainage basin includes areas far from the fault with low rock uplift rates. Conversely, catchments near the fault tips should have abnormally low sediment discharges. This effect should persist until significant fault interaction or linkage occurs, at which time the displacement profile may adjust toward that of a single fault through enhanced displacement rates within the relay zone [*Gupta et al.*, 1998; *Gupta and Scholz*, 2000]. It has been suggested that fracturing near fault tips may locally enhance the erodibility of rocks in relay zones, thus increasing the sediment discharge from these areas [e.g., *Jackson and Leeder*, 1994], although this has not been demonstrated conclusively.

8.4. Fan Size

[44] Finally, the large size and supposedly high sediment discharge from relay zone catchments are commonly cited as evidence for their association with large fan systems. ''Large'' in this context typically implies fans with large surface areas. Following a similar analysis by *Whipple and Trayler* [1996], *Allen and Hovius* [1998] argued that fan area is strongly dependent on fan aggradation rate, which is in turn proportional to sediment supply and inversely proportional to fault displacement rate. We expect that slow rates of fault displacement and base level fall within the relay zone, coupled with the constraints on sediment supply outlined above, are unlikely to facilitate the development of volumetrically large relay zone fans. While relay zone fans may have large surface areas, this may simply be a consequence of low rates of accommodation generation [e.g., *Whipple and Trayler*, 1996; *Allen and Hovius*, 1998; *Allen and Densmore*, 2000]. We suggest that, due to insufficient accommodation, relay zone fans in isolation

are unlikely to be volumetrically significant, although they may have large areas. *Anders and Schlische* [1994] showed that relay zones along several faults in the Basin and Range province are commonly associated with Bouguer gravity highs in the adjacent hanging wall. They interpreted these highs as indicating relatively thin basin deposits adjacent to the relays. However, it is important to note that such analyses cannot identify the source of the sediment in the relay and thus do not directly address the question of sediment supply from relay zone catchments. Adequate fan volume and provenance data are required from a variety of relay zones.

9. Discussion and Conclusions

[45] Catchment erosion and sediment supply in extensional relay zones are likely to be fundamentally controlled by a previously unrecognized competition between two diverse sets of processes (fault array development and the evolution of catchment-fan systems) that operate over potentially very different timescales. The spatial pattern of footwall catchments and hanging wall fans will be dictated, in part, by whether or not the timescale of fault tip propagation and fault array linkage is shorter than, comparable to, or longer than the timescale over which the footwall catchment-fan systems develop. In our experiments, very rapid fault growth leads to widespread stream capture of relay zone drainage area, whereas slow fault tip propagation, in large increments, does not. We also suggest, on the basis of the experimental results and simple physical reasoning, that development of very large catchments in isolated fault blocks is likely to be effectively retarded by space considerations and drainage area competition within the footwall, and that volumetrically large fans are unlikely to occur due to a lack of accommodation and possible diversion of sediment onto the adjacent hanging walls. Interpretation of these results must be tempered by the fact that many other factors, such as fault slip rate, lithology and lithological variations, and climatic change, may also influence the catchment pattern in relay zones but are not simulated here.

[46] This difference in catchment evolutionary history between the two end-member models should result in different patterns of sediment delivery to adjacent hanging wall basins and hence different ages of deposited sediments. Experiment 1 predicts that capture events will lead to abrupt pulses of sediment delivery to the outboard hanging wall as drainage from inboard catchments is rerouted across the outboard footwall. Our simulations predict that these capture-induced sediment pulses will become younger toward the outboard fault tip as capture events migrate toward the tip region as the model evolves (Figure 5). By contrast, in experiment 2 with a propagating tip geometry, no major drainage reorganization or capture events occur, and as a consequence, no abrupt shifts in the loci or rate of sediment delivery to the outboard hanging wall are predicted (Figure 7). Instead, because drainage derived from the inboard footwall becomes etched into the outboard footwall during fault propagation, we predict that sediment delivery to the outboard hanging wall should remain relatively continuous in space and time. Thus a potential test of these end-member models, which cannot be obtained from analysis of the final landscape, may come from the sedimentary architecture and ages of fan sediments in the hanging wall.

[47] Our experiments are limited to normal fault footwalls that evolve in hydrologic isolation, without input of water or sediment from externally sourced, antecedent catchments. How common are these simple systems in extending regions? In the Basin and Range, our qualitative observations suggest that most of the actively deforming ranges are bounded by discrete, geometrically simple faults, which makes them particularly amenable to geomorphic analysis [e.g., *dePolo and Anderson*, 2000]. There are several exceptions to this, particularly in places where the locus of faulting has migrated through time. For example, active faulting along the western margin of the Ruby-East Humboldt Range has migrated westward into the basin [*Sharp*, 1940], while the faults along the western margin of the Tobin Range show evidence of tip propagation and lateral growth [*Jackson and Leeder*, 1994]. In both cases, basinal sediments are now undergoing rock uplift and denudation in the footwalls of the most recently active faults, and so the new footwall drainage systems may be partly inherited. However, for the most part, the ranges in the Basin and Range appear to have evolved as relatively simple, closed footwall systems, in which all available drainage area is contained within the footwall itself. Regional drainages, such as the Humboldt River, the Carson River, or Spring Creek [*Jackson and Leeder*, 1994], are typically axial and flow between widely separated ranges, rather than through small-separation (<10 km) relay zones.

[48] In contrast, basinward migration of fault activity is commonly observed in other extensional settings, leading to inherited catchments and incorporation of basin fill deposits into new fault footwalls. Examples of this behavior have been described from the southern Afar rift [*Hayward and Ebinger*, 1996], central Greece [*Leeder and Jackson*, 1993], and the eastern margin of the Gulf of Suez [*Gupta et al.*, 1999]. *Gupta et al.* [1999] described volumetrically large Miocene fan complexes that developed adjacent to relay zones along the eastern border fault system of the Suez Rift. It seems likely that the footwall drainage systems feeding these fans were inherited regional drainages that used the relay zones as corridors for sediment dispersal, rather than relay catchments consequent on fault overlap. Fan complexes at the margins of other rift basins, e.g., the Upper Jurassic Brae complex in the South Viking Graben, North Sea rift system, may have a similar origin (S. Gupta, unpublished data, 2002).

[49] It may be that antecedent drainage systems are more likely when such migratory fault behavior occurs near the edges of rifts, where a regional basinward slope is present, than when it occurs near the center of rifts or in wide, Basin and Range-style rifts. If true, this would suggest that not all rifts are alike in terms of geomorphic evolution and sediment supply, and that generalization into conceptual models may not be justified. For example, the association of spatially large catchment-fan systems and with zones of fault linkage in the Sperchios Basin, central Greece [*Eliet and Gawthorpe*, 1995] appears to be a consequence of regional drainages being focused through topographically low zones of fault overlap. Catchment size in this field example appears to also have a strong relationship with bedrock lithology; large catchments at fault overlaps are

developed on weak prerift lithologies, in contrast to smaller footwall catchments incised into resistant limestones.

[50] Finally, we return to the issue of competing timescales. If the timescale over which a fault array propagates, interacts, and links is short compared to the time required to develop an organized sediment distribution system in the form of catchments and fans, then most of the basin fill will be insensitive to the details of the fault linkage process. Conversely, if fault linkage occurs over a similar, or longer, timescale to catchment-fan development, then the basin fill should record many of the details of the linkage process. Both of these timescales are potentially long (up to $\sim 10^6$ years) but poorly understood. We suggest that most of the data available at present do not allow us to distinguish between these end-member cases, and indeed generalization to all rifts may not be possible. Research into the precise timescales over which fault arrays have developed in a number of extensional settings is urgently required, as is a better understanding of the implications of fault growth models for surface processes, particularly in terms of spatial and temporal changes in displacement fields. We also note the somewhat surprising lack of quantitative assessments of variations in catchment-fan morphology near relay zones. Detailed three-dimensional (3-D) seismic stratigraphic studies, such as those by *Dawers and Underhill* [2000] and *McLeod et al.* [2000], have shown that, in at least some cases, the overall architecture of basin deposits do shed light on the processes of fault linkage. Future studies of basin evolution must explicitly recognize that sediment supply is not simply fault controlled, but requires the development and maintenance of a complex system of catchments and fans, and that this system has its own inherent length scales and response times [e.g., *Allen and Densmore*, 2000].

[51] **Acknowledgments.** This research was partially supported by an Enterprise Ireland Applied Research Grant in conjunction with Enterprise Oil plc. NHD acknowledges partial support from the Louisiana Board of Regents Support Fund. SG acknowledges partial support from NERC grant GR8/04397. Many thanks to George Hilley, Ramón Arrowsmith, and Manfred Strecker for discussions and for providing us with a preprint of their work. We also thank Patience Cowie, Michael Ellis, Christopher Heltzel, Fritz Schlunegger, Martin Schoepfer, Guy Simpson, and John Walsh for useful discussions and assistance. Reviews by Jean Braun, James Jackson, and an anonymous reviewer greatly improved the focus and organization of the manuscript.

References

Allen, P. A., and A. L. Densmore, Sediment flux from an uplifting fault block, *Basin Res.*, *12*, 367–380, 2000.

Allen, P. A., and N. Hovius, Sediment supply from landslide-dominated catchments: Implications for basin-margin fans, *Basin Res.*, *10*, 19–35, 1998.

Anders, M. H., and R. W. Schlische, Overlapping faults, intrabasin highs, and the growth of normal faults, *J. Geol.*, *102*, 165–179, 1994.

Anders, M. H., M. Spiegelman, D. W. Rodgers, and J. T. Hagstrum, The growth of fault-bounded tilt blocks, *Tectonics*, *12*, 1451–1459, 1993.

Bentham, P., R. E. L. Collier, R. L. Gawthorpe, M. R. Leeder, S. Prosser, and C. Stark, Tectono-sedimentary development of an extensional basin: The Neogene Megara Basin, Greece, *J. Geol. Soc. London*, *148*, 923–934, 1991.

Bürgmann, R., D. D. Pollard, and S. J. Martel, Slip distributions on faults: Effects of stress gradients, inelastic deformation, heterogeneous host-rock stiffness, and fault interaction, *J. Struct. Geol.*, *16*, 1675–1690, 1994.

Cartwright, J. A., B. D. Trudgill, and C. S. Mansfield, Fault growth by segment linkage: An explanation for scatter in maximum displacement and trace length data from the Canyonlands Grabens of SE Utah, *J. Struct. Geol.*, *17*, 1319–1326, 1995.

Cartwright, J. A., C. Mansfield, and B. Trudgill, The growth of faults by segment linkage, in *Modern Developments in Structural Interpretation, Validation and Modelling*, edited by P. G. Buchanan and D. A. Nieuwland, *Geol. Soc. Spec. Publ.*, *99*, 163–177, 1996.

Childs, C., J. Watterson, and J. J. Walsh, Fault overlap zones within developing normal fault systems, *J. Geol. Soc. London*, *152*, 535–549, 1995.

Cowie, P. A., A healing-reloading feedback control on the growth rate of seismogenic faults, *J. Struct. Geol.*, *20*, 1075–1087, 1998.

Cowie, P. A., and C. H. Scholz, Growth of faults by accumulation of seismic slip, *J. Geophys. Res.*, *97*, 11,085–11,095, 1992a.

Cowie, P. A., and C. H. Scholz, Displacement-length scaling relationship for faults: Data synthesis and discussion, *J. Struct. Geol.*, *14*, 1149–1156, 1992b.

Cowie, P. A., and Z. K. Shipton, Fault tip displacement gradients and process zone dimensions, *J. Struct. Geol.*, *20*, 983–997, 1998.

Cowie, P. A., S. Gupta, and N. H. Dawers, Implications of fault array evolution for synrift depocentre development: Insights from a numerical fault growth model, *Basin Res.*, *12*, 241–262, 2000.

Crider, J. G., and D. D. Pollard, Fault linkage: Three-dimensional mechanical interaction between echelon normal faults, *J. Geophys. Res.*, *103*, 24,373–24,391, 1998.

Crossley, R., Controls of sedimentation in the Malawi Rift Valley, central Africa, *Sediment. Geol.*, *40*, 33–50, 1984.

Dawers, N. H., M. H. Anders, and C. H. Scholz, Growth of normal faults: Displacement-length scaling, *Geology*, *21*, 1107–1110, 1993.

Dawers, N. H., and M. H. Anders, Displacement-length scaling and fault linkage, *J. Struct. Geol.*, *17*, 607–614, 1995.

Dawers, N. H., and J. R. Underhill, The role of fault interaction and linkage in controlling synrift stratigraphic sequences: Late Jurassic, Statfjord East area, northern North Sea, *AAPG Bull.*, *84*, 45–64, 2000.

Densmore, A. L., M. A. Ellis, and R. S. Anderson, Landsliding and the evolution of normal fault-bounded mountain ranges, *J. Geophys. Res.*, *103*, 15,203–15,219, 1998.

dePolo, C. M., and J. G. Anderson, Estimating the slip rates of normal faults in the Great Basin, USA, *Basin Res.*, *12*, 227–240, 2000.

Eliet, P. P., and R. L. Gawthorpe, Drainage development and sediment supply within rifts: Examples from the Sperchios basin, central Greece, *J. Geol. Soc. London*, *152*, 883–893, 1995.

Ellis, M. A., A. L. Densmore, and R. S. Anderson, Development of mountainous topography in the Basin Ranges, U.S.A., *Basin Res.*, *11*, 21–41, 1999.

Gawthorpe, R. L., and J. M. Hurst, Transfer zones in extensional basins: Their structural style and influence on drainage development and stratigraphy, *J. Geol. Soc. London*, *150*, 1137–1152, 1993.

Gawthorpe, R. L., and M. R. Leeder, Tectono-sedimentary evolution of active extensional basins, *Basin Res.*, *12*, 195–218, 2000.

Gomberg, J., and M. Ellis, Topography and tectonics of the central New Madrid seismic zone: Results of numerical experiments using a three-dimensional boundary element program, *J. Geophys. Res.*, *99*, 20,299–20,310, 1994.

Gupta, A., and C. H. Scholz, A model of normal fault interaction based on observations and theory, *J. Struct. Geol.*, *22*, 865–879, 2000.

Gupta, S., P. A. Cowie, N. H. Dawers, and J. R. Underhill, A mechanism to explain rift-basin subsidence and stratigraphic patterns through fault array evolution, *Geology*, *26*, 595–598, 1998.

Gupta, S., J. R. Underhill, I. R. Sharp, and R. L. Gawthorpe, Role of fault interaction in controlling synrift dispersal patterns: Miocene, Abu Alaqa Group, Suez Rift, Sinai, Egypt, *Basin Res.*, *11*, 167–189, 1999.

Hancock, G. S., R. S. Anderson, and K. X. Whipple, Beyond power: Bedrock river incision process and form, in *Rivers Over Rock: Fluvial Processes in Bedrock Channels*, *Geophys. Monogr. Ser.*, vol. 107, edited by K. J. Tinkler and E. E. Wohl, pp. 35–60, AGU, Washington, D.C., 1998.

Hardy, S., and R. L. Gawthorpe, Bedrock channel incision and sediment supply in extensional basins: Insights from numerical modelling, *Eos Trans. AGU*, *81*(48), Fall Meet. Suppl., Abstract T71E-03, 2000.

Hayward, N. J., and C. J. Ebinger, Variations in the along-axis segmentation of the Afar Rift system, *Tectonics*, *15*, 244–257, 1996.

Huggins, P., J. Watterson, J. J. Walsh, and C. Childs, Relay zone geometry and displacement transfer between normal faults recorded in coal-mine plans, *J. Struct. Geol.*, *17*, 1741–1755, 1995.

Jackson, J., and M. R. Leeder, Drainage systems and the development of normal faults: An example from Pleasant Valley, Nevada, *J. Struct. Geol.*, *16*, 1041–1059, 1994.

Jackson, J. A., and N. J. White, Normal faulting in the upper continental crust: Observations from regions of active extension, *J. Struct. Geol.*, *11*, 15–36, 1989.

Larsen, P.-H., Relay structures in a Lower Permian basement-involved extension system, East Greenland, *J. Struct. Geol.*, *10*, 3–8, 1988.

Leeder, M. R., and R. L. Gawthorpe, Sedimentary models for extensional tilt-block/half-graben basins, in *Continental Extensional Tectonics*, edited

by M. P. Coward, J. F. Dewey, and P. L. Hancock, *Geol. Soc. Am. Spec. Publ.*, *28*, 139–152, 1987.

Leeder, M. R., and J. A. Jackson, The interaction between normal faulting and drainage in active extensional basins, with examples from the western United States and central Greece, *Basin Res.*, *5*, 79–102, 1993.

McCalpin, J. P., Neotectonic deformation along the East Cache fault zone, Cache County, Utah, *Utah Geol. Min. Surv. Spec. Stud.*, *83*, 37 pp., 1994.

McLeod, A. E., N. H. Dawers, and J. R. Underhill, The propagation and linkage of normal faults: Insights from the Strathspey-Brent-Statfjord fault array, northern North Sea, *Basin Res.*, *12*, 263–284, 2000.

Morewood, N. C., and G. P. Roberts, Lateral propagation of the surface trace of the South Alkyonides normal fault segment, central Greece: Its impact on models of fault growth and displacement-length relationships, *J. Struct. Geol.*, *21*, 635–652, 1999.

Morley, C. K., Patterns of displacement along large normal faults: Implications for basin evolution and fault propagation, based on examples from East Africa, *AAPG Bull.*, *83*, 613–634, 1999.

Peacock, D. C. P., and D. J. Sanderson, Displacements, segment linkage and relay ramps in normal fault zones, *J. Struct. Geol.*, *13*, 721–733, 1991.

Ravnås, R., and R. J. Steel, Architecture of marine rift-basin successions, *AAPG Bull.*, *82*, 110–146, 1998.

Schlische, R. W., Half-graben basin filling models: New constraints on continental extensional basin development, *Basin Res.*, *3*, 123–141, 1991.

Schlische, R. W., S. S. Young, R. V. Ackermann, and A. Gupta, Geometry and scaling relations of a population of very small rift-related normal faults, *Geology*, *24*, 683–686, 1996.

Sharp, R. P., Geomorphology of the Ruby-East Humboldt Range, Nevada, *Geol. Soc. Am. Bull.*, *51*, 337–371, 1940.

Sklar, L., and W. E. Dietrich, River longitudinal profiles and bedrock incision models: Stream power and the influence of sediment supply, in *Rivers Over Rock: Fluvial Processes in Bedrock Channels*, *Geophys. Monogr. Ser.*, vol. 107, edited by K. J. Tinkler and E. E. Wohl, pp. 237–260, AGU, Washington, D.C., 1998.

Stein, R. S., G. C. King, and J. B. Rundle, The growth of geological structures by repeated earthquakes: 2. Field examples of continental dip-slip faults, *J. Geophys. Res.*, *93*, 13,319–13,331, 1988.

Strecker, M. R., G. E. Hilley, J. R. Arrowsmith, and I. Coutand, Differential structural and geomorphic mountain-front evolution in an active continental collision zone: the northwest Pamir, southern Kyrgystan, *Geol. Soc. Am. Bull.*, *115*, 166–181, 2003.

Trudgill, B., and J. Cartwright, Relay ramp forms and normal fault linkages, Canyonlands National Park, Utah, *Bull. Geol. Soc. Am.*, *106*, 1143–1157, 1994.

Wallace, R. E., Fault-plane segmentation in brittle crust and anisotropy in loading system, in *Proceedings of Conference XLV; A Workshop on Fault Segmentation and Controls of Rupture Initiation and Termination*, edited by D. P. Schwartz and R. H. Sibson, *U.S. Geol. Surv. Open File Rep., 89-0315*, 400–408, 1989a.

Wallace, R. E., Geometry and rates of change of fault-generated range fronts, north-central Nevada, *J. Res. U.S. Geol. Surv.*, *6*, 637–649, 1989b.

Walsh, J. J., and J. Watterson, Geometric and kinematic coherence and scale effects in normal fault systems, in *The Geometry of Normal Faults*, edited by A. M. Roberts, G. Yielding, and B. Freeman, *Geol. Soc. Spec. Publ.*, *56*, 193–203, 1991.

Whipple, K. X., and C. R. Trayler, Tectonic control of fan size: The importance of spatially variable subsidence rates, *Basin Res.*, *8*, 351–366, 1996.

Whipple, K. X., and G. E. Tucker, Dynamics of the stream-power river incision model: Implications for height limits of mountain ranges, landscape response timescales, and research needs, *J. Geophys. Res.*, *104*, 17,661–17,674, 1999.

Whipple, K. X., G. S. Hancock, and R. S. Anderson, River incision into bedrock: Mechanics and relative efficacy of plucking, abrasion, and cavitation, *Geol. Soc. Am. Bull.*, *112*, 490–503, 2000.

Willemse, E. J. M., D. D. Pollard, and A. Aydin, 3D analyses of slip distributions on normal fault arrays with consequences for fault scaling, *J. Struct. Geol.*, *18*, 295–309, 1996.

Willett, S. D., and M. T. Brandon, On steady states in mountain belts, *Geology*, *30*, 175–178, 2002.

Wu, D., and R. L. Bruhn, Geometry and kinematics of active normal faults, South Oquirrh Mountains, Utah: Implication for fault growth, *J. Struct. Geol.*, *16*, 1061–1075, 1994.

P. A. Allen and A. L. Densmore, Institute of Geology, Department of Earth Sciences, ETH Zentrum, CH-8092 Zürich, Switzerland. (philip.allen@erdw.ethz.ch; densmore@erdw.ethz.ch)

N. H. Dawers, Department of Geology, Tulane University, New Orleans, LA 70118, USA. (ndawers@tulane.edu)

R. Gilpin, Department of Geology and Geophysics, University of Edinburgh, West Mains Road, Edinburgh EH9 3JW, UK. (gilpinr@glg.ed.ac.uk)

S. Gupta, Department of Earth Sciences and Engineering, South Kensington Campus, Imperial College, London SW7 2AZ, UK. (s.gupta@ic.ac.uk)